



HAL
open science

Linking soil moisture sensors and crop models for irrigation management

Antoine Haddon, Loïc Kechichian, Jérôme Harmand, Cyril Dejean, Nassim Ait-Mouheb

► **To cite this version:**

Antoine Haddon, Loïc Kechichian, Jérôme Harmand, Cyril Dejean, Nassim Ait-Mouheb. Linking soil moisture sensors and crop models for irrigation management. *Ecological Modelling*, 2023, 484, pp.110470. 10.1016/j.ecolmodel.2023.110470 . hal-03909071

HAL Id: hal-03909071

<https://hal.inrae.fr/hal-03909071v1>

Submitted on 21 Dec 2022

HAL is a multi-disciplinary open access archive for the deposit and dissemination of scientific research documents, whether they are published or not. The documents may come from teaching and research institutions in France or abroad, or from public or private research centers.

L'archive ouverte pluridisciplinaire **HAL**, est destinée au dépôt et à la diffusion de documents scientifiques de niveau recherche, publiés ou non, émanant des établissements d'enseignement et de recherche français ou étrangers, des laboratoires publics ou privés.

1 Linking soil moisture sensors and crop models for irrigation 2 management

3
4 Antoine Haddon^{*a}, Loïc Kechichian^b, Jérôme Harmand^a, Cyril Dejean^b, Nassim Ait-Mouheb^b

5
6 ^aINRAE, Univ Montpellier, LBE, 102 Avenue des Etangs, Narbonne, France.

7 ^bINRAE, Univ Montpellier, UMR GEAU, Montpellier, France.

8 ^{*}Corresponding author (antoine.haddon@inrae.fr)

9 10 11 **Abstract**

12 A number of challenges must be faced when using soil moisture sensors, such as
13 accounting for soil heterogeneity in measurements or dealing with sensor faults. As a
14 consequence, it is difficult to obtain reliable estimations of the water status in the root zone
15 and using sensor data for irrigation planning is not straightforward. In this work, a method is
16 proposed to interpret soil water content measurements that is based on the use of a model
17 to correct and complement sensor data, in particular in the case of a non uniform water
18 distribution. This approach relies on the assumption that porosity is the main driver of
19 heterogeneity in hydraulic properties at small scales, which allows to factor out the spatial
20 variations of the sensor's signal. With practical applications in mind, a simple model and an
21 efficient calibration procedure are developed, in particular considering the online application
22 of the method to complement sensor data in real time. The capabilities of the model are
23 illustrated with data from experiments on the growth of lettuces in greenhouses with
24 reclaimed wastewater irrigation. Requiring only a short calibration period, the model is
25 successfully validated and is proven to be a valuable tool to correct for sensor malfunctions.
26 Moreover, the proposed method is shown to allow the meaningful estimation of the water
27 status of the soil crop system, in particular when measurements of sensors positioned close
28 to each other showed important differences.

29
30 **Keywords:** soil water sensor ; simplified model ; irrigation scheduling

31 32 33 **1 Introduction**

34
35 Increasing water scarcity and the essential role irrigation plays in food security in many
36 regions of the world, calls for a better management of water uses in agriculture. A key
37 element of any efficient irrigation system that is capable of achieving high yields, is the
38 appropriate planning of water inputs to meet the crops needs. This requires answering two
39 questions : when irrigation should be triggered and how much water needs to be applied. To
40 help in taking these decisions, different approaches have been used and often rely on
41 information on the water status and dynamics of the soil-crop system either through the use
42 of sensors or with models incorporating weather data (Abioye 2020, Villalobos 2016).

43
44 Sensors have been developed that allow the measurement of the soil water content (SWC)
45 or the water potential and have been used independently of models for irrigation planning.
46 Typically, in this case, the decision to irrigate is taken when a certain threshold is reached,
47 which represents the onset of plant water stress. Then, to avoid excess irrigation and

48 compute the appropriate irrigation volume it is necessary to also know the soil field capacity.
49 However, determining the irrigation threshold value and the field capacity for a given soil
50 remains challenging (Vories 2021). Appropriate sensor calibration also represents a
51 difficulty, with various effects impacting sensors, such as temperature, that must be
52 compensated (Feng 2020). Cheaper sensors have been introduced to reduce costs but
53 these are less reliable, with sensor faults that lead to corrupted data, further complicating the
54 use of sensors for irrigation (Bogena 2007). Nonetheless, among the issues that have been
55 reported with using sensors for irrigation scheduling, the interpretation of sensor data has
56 been considered as the main difficulty (Sui 2020). In particular, a number of problems arise
57 from a non uniform distribution of water in the soil, since spatial variations in SWC makes it
58 challenging to determine if the sensor output actually represents the water status of the root
59 zone. As a result, the positioning of sensors has an important impact on measurements, with
60 differences observed in sensors over short distances (Bogena 2007, Vories 2021).

61
62 Approaches for irrigation planning based on models include water balance methods, which
63 use weather data along with a model to estimate evapotranspiration losses, and compute
64 irrigation to compensate (Allen 1998, Villalobos 2016, Pereira 2020). From the first simple
65 models, more complex dynamic models have been developed, with detailed soil water
66 balances to estimate the distribution of water in the soil column (Brisson 2003, Rodríguez-
67 Iturbe 2007, Mailhol 2011, Cheviron 2016, Šimůnek 2018). However, a more detailed
68 representation of the water dynamics leads to increased complexity and models that are
69 harder to use, with calibration of model parameters representing a serious difficulty for the
70 most complex models. This is an important consideration for a model that must be used in
71 practice, as a model must first be calibrated to be applied to each specific situation.

72
73 Combining both models along with sensors is an interesting solution to overcome the
74 shortcomings of each approach when used separately. On one hand, sensors offer the
75 possibility to link models to reality, with sensor data used for the calibration of models.
76 On the other hand, models can be used to correct sensor output in the case of faults but also
77 allows the integration of weather and sensor data to gain a broader perspective and a better
78 understanding of a specific irrigation problem. In addition, this opens the possibility for the
79 use of a wide variety of tools from monitoring and control engineering for irrigation
80 management (Abioye 2020, Cobbenhagen 2021). However, this raises the often overlooked
81 issue of linking sensors and models and how to assimilate data from sensors into models. In
82 particular, due the difficulties in interpreting sensor data, it is not straightforward to establish
83 a correspondence between sensor output and model variables. In this work, we focus on the
84 problems associated with the non uniform distribution of soil water content, and how to deal
85 with soil heterogeneity when using sensor data along with a model. In section 2, we present
86 a model, explaining the link between sensor output and model variables and then we detail a
87 parameter calibration procedure specifically developed. This approach is tested with
88 experimental data, presented in section 3. Results are discussed in section 4 before
89 conclusions in section 5.

90 91 **2 Model Presentation**

92 *2.1 Soil water content*

93 Variations in the distribution of water in the soil are caused by a number of factors, which
94 have impacts at different scales. In an area exposed to similar conditions, differences in
95 SWC can be the result of heterogeneities in soil composition and structure (Warrick 2001).

96 Soil composition, i.e. mineral particle size distribution and organic matter content, can vary at
97 the scale of a field but locally, such as near a sensor, it is reasonable to consider it constant.
98 Spatial variations in SWC can be the result of heterogeneities in the soil structure, in
99 particular the porosity, and this can occur at a small scale. Indeed, differences in soil
100 compaction will lead to variations in the distribution of pores, affecting the water holding
101 capacity and the entire soil water dynamics.

102
103 In this study, the measurement of SWC from sensors based on capacitance and frequency
104 domain reflectometry technology are considered. These rely on the relation between the
105 SWC and the dielectric permittivity of the soil due to the different permittivities of water,
106 minerals and air. In turn, capacitance is related to the permittivity of the medium surrounding
107 the sensors, and therefore capacitance can be used to indirectly measure SWC. The output
108 of these sensors is then converted through a regression curve to the volumetric soil water
109 content (VWC), which is the ratio of the water volume relative to the total volume :

$$111 \theta = \frac{WaterVolume}{TotalVolume} \quad (1)$$

112
113 The total volume of soil can be decomposed into the volume of solid components and the
114 pore volume, which itself is composed of the volume of air and water. As a consequence,
115 porosity will thus impact the sensor's measurements and in particular, a spatial
116 heterogeneity of porosity will result in variations of VWC. Typically, if two sensors are
117 positioned close by in an area where the soil water status should be the same, the sensors
118 can output different measurements due to small variations of porosity. This raises the issue
119 of interpreting sensor data and in particular the validity of a measurement for a given area.

120
121 As a consequence, using sensor data along with a model for irrigation planning requires
122 some methodology to account for the local spatial variations in soil water measurements.
123 One possibility is to use a model with variables for soil water expressed as VWC and to
124 represent soil heterogeneity in detail. This is the approach followed by many dynamic soil
125 and crop models, and this leads to considering a fine representation of the soil to compute in
126 detail the distribution of water (Brisson 2003, Šimůnek 2018). However, with this approach,
127 soil heterogeneity is represented by varying the parameters associated with the different soil
128 properties. Indeed, the characteristic moisture levels, such as field capacity or wilting point,
129 when expressed in VWC, would have to be different at various points in space to reflect the
130 variations of soil structure. In particular, this raises the issue of the calibration of these
131 distributed parameters, which are functions of space. At least, it would be necessary to
132 calibrate, for each sensor position, all the parameters representing characteristic soil
133 moisture levels, such as field capacity and wilting point.

134
135 The complexity of this approach and the associated models can be questioned in practical
136 applications, where model usability and efficiency are important. Furthermore, models for
137 decision support do not necessarily need to be as detailed as those developed for scientific
138 purposes, in particular if they are to be used by farmers. For the problem studied here, the
139 limited online measurements from a few sensors and the little information on the soil
140 properties available in practice make it difficult to accurately calibrate complex models and
141 justify the use of simpler models.

142

143 Instead, the model and the associated calibration method proposed here consider soil water
144 variables expressed as Pore Water Content (PWC), which is the soil water volume relative to
145 pore volume :

$$146 \quad S = \frac{\text{WaterVolume}}{\text{PoreVolume}} \quad (2)$$

148 Porosity ϕ is defined as the ratio of pore volume to total volume,

$$149 \quad \phi = \frac{\text{PoreVolume}}{\text{TotalVolume}} \quad (3)$$

152 Therefore, PWC and VWC are related by

$$153 \quad \theta = \phi S \quad (4)$$

156 Then, sensor data, which is recorded as VWC, can be readily converted to PWC once
157 porosity has been estimated.

159 The choice of using PWC variables is based on the hypothesis that the local variations in soil
160 water content are the result of local differences in soil porosity. Furthermore, we make the
161 assumption that the VWC measurements can be decomposed according to (4) into the
162 product of porosity, which represents the soil's spatial heterogeneity, and PWC, which is
163 assumed to be constant locally. In other words, we suppose that the sensor output $\theta(t, x)$
164 which varies in space and time, is the product of a term which varies only in space, porosity
165 $\phi(x)$, and another term which varies only in time, PWC $S(t)$:

$$166 \quad \theta(t, x) = \phi(x)S(t) \quad (5)$$

169 with x representing a space coordinate and t the time coordinate.

171 An important advantage of this approach is that it does not require a fine representation of
172 the soil and instead the variables of PWC will represent the water content in a large area
173 where soil type is constant. This results in an efficient model with only a few variables.
174 Furthermore, the porosity is the only parameter used to account for differences in recorded
175 VWC and is calibrated to the sensor data. Indeed, it is assumed that, when expressed as
176 PWC, the characteristic soil moisture levels depend only on the soil type but not on the
177 porosity. Thus, considering that the soil type is homogenous in an area results in constant
178 characteristic soil moisture levels. The associated parameters can therefore be set from
179 reference values based on the soil composition. This method has the advantage of requiring
180 the calibration of only one parameter per sensor to explain the spatial variations and this is
181 important in obtaining an efficient and generic calibration method.

183 To justify these hypotheses, first note that characteristic soil moisture levels, when they are
184 expressed as levels of soil water potential, can be considered to be independent of soil
185 porosity or composition (Laio, 2001). For example, the wilting point is assumed to
186 correspond to a soil water potential of -3 MPa, with variations essentially due to plant type
187 but not due to soil composition or porosity. Next, a soil water retention curve can be used to

189 convert water potential to VWC and in particular the following relation has been proposed
190 (Clapp 1978),

$$192 \left(\frac{\psi}{\psi_s}\right)^b = \frac{\theta}{\phi} \quad (6)$$

193
194 Here, ψ is the soil water potential, ψ_s and b are parameters depending on the soil type. The
195 water retention curve therefore encapsulates the different sources of spatial variation in
196 water content due to soil type and porosity. Note that VWC and PWC are related through
197 porosity and can be rewritten to relate the soil water potential to PWC:

$$199 \left(\frac{\psi}{\psi_s}\right)^b = S \quad (7)$$

200
201 The important observation here is that this relation is independent of porosity. The
202 consequence is that, if the characteristic soil moisture levels correspond to constant soil
203 water potentials, then they do not vary with porosity when they are expressed as PWC. For
204 example, assuming that the soil water potential at the wilting point and the soil type are
205 constant in a given area implies that the wilting point is also constant when expressed in
206 PWC. Note however that the parameters ψ_s and b vary with soil composition and thus this
207 gives the dependence on soil type of the PWC characteristic soil moisture levels.

208

209 *2.2 Model dynamics*

210 The model proposed here is a soil water balance compartment model, each compartment
211 corresponding to a layer of soil in an area around a sensor. The main variables are the soil
212 water content, expressed in PWC, and are assumed to represent soil water content of the
213 area surrounding each sensor where the soil composition is constant. The horizontal
214 movement of water is neglected and therefore areas of different soil composition are not
215 connected. However, to represent vertical variation and movement of water, several layers
216 can be considered as a series of interconnected compartments. The number of layers
217 depends on the number of sensors used and can be adapted to the crop and soil type, with
218 the case of crops with deep roots or vertically heterogeneous soils requiring more layers.
219 The model developed here considers a division of the soil column in 2 layers, with the
220 objective of using data from sensors positioned at 2 different depths.

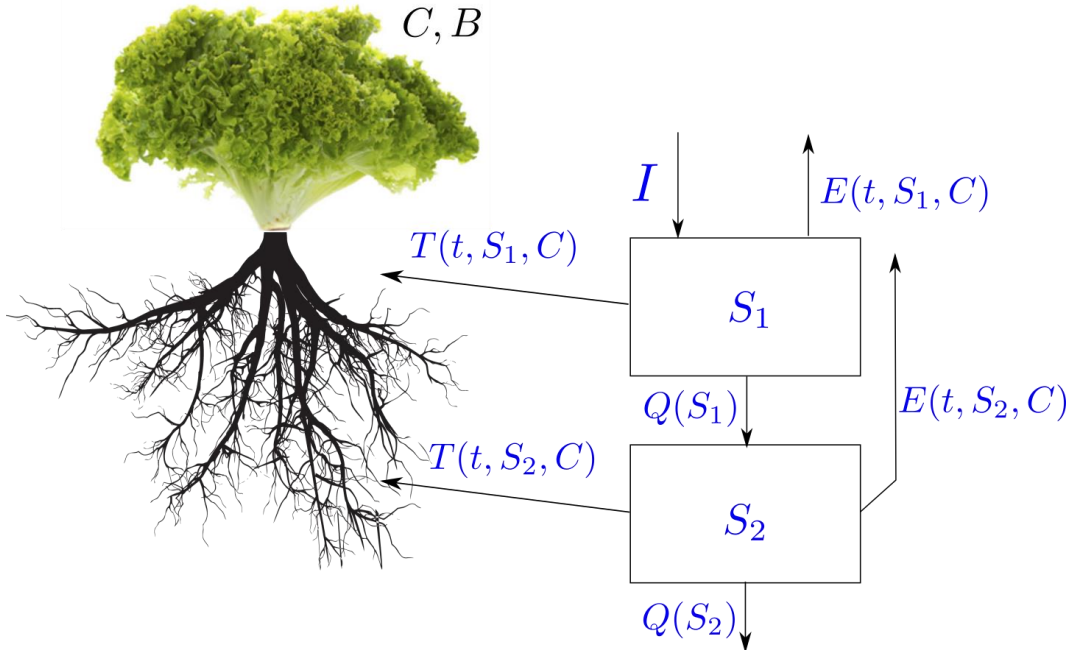
221

222 The dynamics are obtained by considering the balance of inputs and outputs in each
223 compartment. Unlike many crop models that use a fixed time step, the model presented here
224 considers a continuous time, which is better suited to capture phenomena with different
225 timescales such as those present in the soil water dynamics. The result is a continuous
226 dynamical system described by a set of ordinary differential equations. The choice of this
227 approach also allows to take advantage of the tools developed in dynamical systems theory,
228 such as observer and control methods (Khalil, 2015).

229

230 To compute losses due to evapotranspiration, crop growth is computed and the model
231 presented here uses concepts originated in the methods of the FAO Irrigation and Drainage
232 Paper No. 56 (Allen 1998) and further developed in the AquaCrop model (Steduto 2009).
233 Such concepts have already been applied to construct continuous dynamical systems crop
234 models (Laio, 2001, Rodríguez-Iturbe 2007, Pelak 2017). The model presented here largely

235 follows these works but with a few modifications. In particular, only vertically homogeneous
 236 soils had been considered and here these models are extended to the multi-layer case.
 237
 238



239 *Figure 1: Schematic representation of the 2 layer model. S_i is the pore water content (PWC)*
 240 *of layer i , C canopy cover, B biomass, I irrigation, E evaporation, T transpiration and Q*
 241 *leakage.*

242
 243

244 The model variables are the PWC in the top layer S_1 , and in the bottom layer S_2 . The crop is
 245 represented with the above ground dry biomass B [kg m^{-2}] and canopy cover C , which is the
 246 fraction of ground shaded by the canopy.

247

248 Denoting Z_i the height and ϕ_i the porosity of the layer i (with $i = 1$ or 2), then $\phi_i Z_i$ represents
 249 the active depth, *i.e.* the volume per unit area of pore space in the considered layer.

250 Therefore $\phi_i Z_i S_i$ is the height of water of the layer and is the quantity on which the balance
 251 is written, considering input from irrigation I and losses due to transpiration T , evaporation E
 252 and drainage Q .

253

$$254 \quad \phi_1 Z_1 \frac{dS_1}{dt}(t) = I(t) - T(t, S_1, C) - E(t, S_1, C) - Q(S_1) \quad (8)$$

$$255 \quad \phi_2 Z_2 \frac{dS_2}{dt}(t) = Q(S_1) - T(t, S_2, C) - E(t, S_2, C) - Q(S_2) \quad (9)$$

256

257 The soil water balance follows the dual crop coefficient method and uses the canopy cover
 258 to partition the Penman-Monteith reference evapotranspiration ET_0 into transpiration and
 259 evaporation. Then the transpiration flux, from layer $i = 1$ or 2 , is computed as:

260

$$261 \quad T(t, S_i, C) = K_{cb}^i K_S(S_i) CET_0(t) \quad (10)$$

262

263 with K_{cb}^i the crop transpiration coefficient and K_S the water stress function.

264

$$K_S(S) = \begin{cases} 0 & \text{for } S \leq S_w \\ \frac{S-S_w}{S^*-S_w} & \text{for } S_w < S \leq S^* \\ 1 & \text{for } S^* < S \end{cases} \quad (11)$$

266
267 with S_w the wilting point and S^* the water stress level.

268
269 For simplicity and to obtain a parsimonious model, several processes are not explicitly
270 represented in this model, as for instance root growth. Limited root growth could limit
271 transpiration, in particular in the early stages of plant life, but it is considered here that this
272 effect is indirectly taken into account through the presence of the canopy cover in the
273 expression of transpiration which already limits the crops' water consumption. In addition, a
274 difference in root density between the 2 layers could change the transpiration flux from each
275 layer but this is accounted for by taking different crop transpiration coefficients K_{cb}^i in each
276 layer.

277
278 Similarly, the evaporation flux from layer $i=1$ or 2 is computed as:

$$E(t, S, C) = K_e^i K_r(S) (1 - C) E T_0(t) \quad (12)$$

281
282 with K_e^i the evaporation coefficient and K_r the evaporation reduction function.

$$K_r(S) = \begin{cases} 0 & \text{for } S \leq S_h \\ \frac{S-S_h}{1-S_h} & \text{for } S_h < S \leq 1 \end{cases} \quad (13)$$

285
286 The two layers are connected through the leakage term, with the water draining from the top
287 layer $Q(S_1)$ feeding into the bottom layer. Leakage is modelled with a tipping bucket
288 approach, with no flow when PWC is less than field capacity S_{fc} ,

$$Q(S) = \begin{cases} 0 & \text{for } S \leq S_{fc} \\ k_{sat} \frac{S-S_{fc}}{1-S_{fc}} & \text{for } S_{fc} < S \leq 1 \end{cases} \quad (14)$$

291
292 with k_{sat} the saturation conductivity.

293
294 A logistic equation is considered for the canopy cover and the growth rate is proportional to
295 crop transpiration, to account for limitations in case of water stress.

$$\frac{dc}{dt}(t) = r_G (T(t, S_1, C) + T(t, S_2, C)) \left(1 - \frac{C}{C_{max}}\right) \quad (15)$$

299
300 with r_G the potential canopy growth rate and C_{max} the maximum canopy cover.

301
302 Biomass growth follows the concept of water productivity used in Aquacrop, with growth
303 proportional to the total transpiration flux,

304

305
$$\frac{dB}{dt}(t) = W_* \frac{T(t,S_1,C)+T(t,S_2,C)}{ET_0(t)} \quad (16)$$

306

307 with W_* the daily water productivity.

308

309 The model considered is thus composed of equations (8), (9), (15), (16) and schematically
310 represented in Figure 1.

311

312 The model can be used to compute the total water losses due to evaporation, transpiration
313 and leakage over a given time interval $[0,T]$:

314 Total Evaporation : $\int_0^T E(t, S_1, C) + E(t, S_2, C) dt$

315 Total Transpiration : $\int_0^T T(t, S_1, C) + T(t, S_2, C) dt$

316 Total Leakage : $\int_0^T Q(S_2) dt$

317

318

319 *2.3 Parameter calibration*

320 The model parameters can either be set from reference values from public databases,
321 directly measured or estimated from available sensor data. The latter case requires solving
322 the optimisation problem of minimising the error between model simulations and
323 measurement data. This can be computationally intensive and present a number of
324 challenges, such as the problem of identifiability (Walter 1997). For these reasons, it is
325 important to set as many parameters as possible by other means to obtain an efficient
326 calibration.

327

328 Table 1 lists the parameters set from references. As previously explained, the parameters
329 representing soil hydraulic properties (characteristic soil moisture levels S_h, S_w, S_*, S_{fc} and the
330 saturated conductivity k_{sat}) values are selected based on the soil type which can be
331 identified with granulometric measurements. Values of these characteristic soil moisture
332 levels in PWC for different soil types can be found in (Laio, 2001). The parameter C_{max}
333 represents the maximum area of the soil surface that can be shaded by the crops canopy
334 and therefore depends on the plant type as well as geometric consideration, such as row
335 spacing.

336

337 The height Z_i of each compartment can be set by first considering that the modelled soil
338 layers correspond to a compartment where the water content or soil type does not vary
339 considerably. In addition, sensors have a given volume of influence and measurements
340 correspond to an average over this volume. Therefore, with the objective of reproducing
341 sensors data, the heights Z_i should be related to the vertical size of the volume of influence
342 of the soil moisture sensors. Accordingly, knowledge of the soil column composition, its
343 variation and the properties of the sensors should be taken into account in positioning
344 sensors and setting the height parameters Z_i .

345

346 All other parameters (Table 2) are calibrated by minimising the error between simulations
347 and measurement data. The root mean square (RMSE) is used to compute errors :

348

349 $RMSE = \sqrt{\frac{1}{N} \sum_{k=1}^N (D_k - X(t_k))^2}$

350 (17)

351 with N the number of data points, D_k the measured data at time t_k and $X(t_k)$ the simulated
 352 value. When combining several variables expressed in different units (i.e. PWC and canopy
 353 cover), errors are computed by summing the relative RMSE (relRMSE) for each variable :

354

355 $relRMSE = \frac{RMSE}{\bar{D}}$ (18)

356

357 with \bar{D} the mean of the data.

358

359 The porosity ϕ_i is the main parameter that must be calibrated as it is considered here to
 360 account for the spatial variability of soil properties. Several sets of sensors can be used to
 361 monitor the soil for redundancy purposes or to study variations between different areas. In
 362 these cases, the porosity must be estimated for each soil water sensor. When sensors are
 363 used over several growth cycles, if the soil surrounding the sensors is left undisturbed, the
 364 same parameters can be used for a new growth cycle. However, if the sensor is positioned
 365 in proximity to roots or if the soil is disturbed due to tillage between growth cycles, then the
 366 soil structure will change and thus porosity must be estimated again.

367

368 The other calibrated parameters are independent of individual sensor's and it is possible to
 369 use the same parameters for different sets of sensors. However, the use of the same set of
 370 parameters over several production cycles or if the growing conditions are different is limited.
 371 Indeed, due to the simplicity of the model considered here, a number of effects are not taken
 372 into account and instead the impact of processes not represented end up hidden in
 373 parameters. For example, the impact of temperature on crop growth is only taken indirectly
 374 into account through reference evapotranspiration but it has been known for a long time that
 375 biomass growth depends on temperature, with the concept of growing degree days. For this
 376 model, this means that the biomass growth rate in fact depends on temperature. As a
 377 consequence it is necessary to re-calibrate parameters for different production cycles or if
 378 growing conditions change, depending on the role of each parameter. Table 2 lists the
 379 circumstances for which each parameter must be calibrated.

380

381 In practice, due to the importance of the porosity on the water dynamics, this parameter can
 382 be first estimated alone, to get a preliminary ajustement of the general features of the soil
 383 water dynamics. Then, the precise calibration is conducted in a second step, with the
 384 estimation at the same time of the porosity along with the evapotranspiration and canopy
 385 growth rate parameters to get a precise fit for the S and C variables. This is the step that is
 386 the most challenging, as it can require the estimation of up to 7 parameters and thus there is
 387 a strong interest in reusing parameters from a previous calibration if possible. Finally, as the
 388 biomass does not affect the dynamics of other variables in the model presented here, the
 389 growth rate (W_*) can be estimated independently at the end to obtain a good adjustment of
 390 the biomass.

391

392

393 *Table 1 : Model parameters, set from references*

Parameter	Value	Units	Name	Source
Z_i	100	mm	Depth of layer i	METER Group
S_h	0.19	-	Hygroscopic point	Laio, 2001
S_W	0.24	-	Wilting point	Laio, 2001
S^*	0.57	-	Point of incipient stomatal closure	Laio, 2001
S_{fc}	0.65	-	Field capacity	Laio, 2001
k_{sat}	200	mm/d	Saturated hydraulic conductivity	Laio, 2001
C_{max}	0.8	-	Maximum canopy cover	-

394
395
396

Table 2 : Model parameters, calibrated from data.

Parameter	Units	Name	Calibration
ϕ_i	-	Porosity	For each sensor
K_{cb}^i	-	Transpiration crop coefficient	For each production cycle
K_e^i	-	Evaporation crop coefficient	For each soil type
r_G	1/d	Canopy cover growth rate	For each production cycle and growing condition
W^*	kg m ² /d	Normalised daily water productivity	For each production cycle

397
398
399
400
401
402
403
404
405
406
407
408
409
410
411
412
413
414
415
416
417
418
419

3 Calibration and validation data

The approach presented here is illustrated in the context of experiments in wastewater reuse, in which irrigation with freshwater and reclaimed water is compared. This offers the possibility to showcase the use of a model for the interpretation and correction of sensor measurements. Furthermore, this allows to demonstrate the capabilities of the model and the associated calibration procedure in different growing conditions. It should be noted that the quantitative control of treated wastewater reuse in agriculture is an important issue, considering that it is a resource that can be limited and moreover to avoid possible sanitary and agronomic impacts of uncontrolled wastewater irrigation (Ait-Mouheb et al. 2018).

3.1 Experimental site

The experimental site is located at Murviel-lès-Montpellier, in the south of France (43.605° N 3.757° E), on a wastewater treatment plant which is equipped with a constructed wetland, composed of reed bed filters with forced aeration, and with additional secondary treatment with ferric chloride as flocculant to remove phosphorus. Two greenhouses of 100 m² each have been in use since 2017, to run experiments on the impact of wastewater reuse in agriculture (Ait-Mouheb et al. 2022). Large soil bins (1m² and 60 cm soil depth) are used to isolate the experiments and avoid field contamination resulting from irrigation with reclaimed wastewater. The bins were filled with loamy clay soil (24.5% clay, 32% fine silt, 13.7% silt, 10.6% fine sand and 19.2 % of sand).

420 Lettuces (*Lactuca sativa*) were grown in 2021, with 8 plants per bin and starting with
421 plantlets at the 3 leaf stage. Two growth cycles of 6 weeks were conducted, from 13 April to
422 25 May and from 27 May to 5 July, hereafter referred to as cycle 1 and cycle 2, respectively.
423 Meteorological variables were measured with a weather station located in the greenhouse.
424 Hourly air temperature, relative humidity and global radiation levels were recorded during
425 both growth cycles.

426

427 *3.2 Irrigation and fertilisation*

428 The bins were irrigated with different water qualities and in this study we focus on the 2 bins
429 in which soil moisture sensors were positioned, with one bin irrigated with freshwater (FW)
430 and another with treated wastewater (TWW). Drip irrigation was conducted with one surface
431 dripper per lettuce and one dripper without any plant in the centre of the bin. The drippers
432 deliver a nominal flow rate of 2 L/h and flow rates were monitored during the irrigation cycles
433 and showed no significant variation. According to the manufacturer's recommendations,
434 irrigation water was filtered at 130 µm before irrigation to prevent physical clogging of the
435 drippers.

436

437 Irrigation was performed twice a week during cycle 1 and 3 times per week during cycle 2,
438 with irrigation volumes computed to compensate for evapotranspiration and guarantee a
439 VWC above 0.15. Evapotranspiration was estimated using the method from the Food and
440 Agricultural Organization of the United Nation (FAO) Irrigation and Drainage Paper No. 56
441 (Allen 1998). First, reference evapotranspiration ET_0 was computed from weather data with
442 the Penman-Monteith equation. Then, evapotranspiration was computed as:

443

$$444 \quad ET = K_c ET_0 \quad (19)$$

445

446 using a crop coefficient $K_c = 0.4$ from germination to 18 leafs and then $K_c = 0.8$ from 18
447 leaves to harvest (Berry, 2013).

448

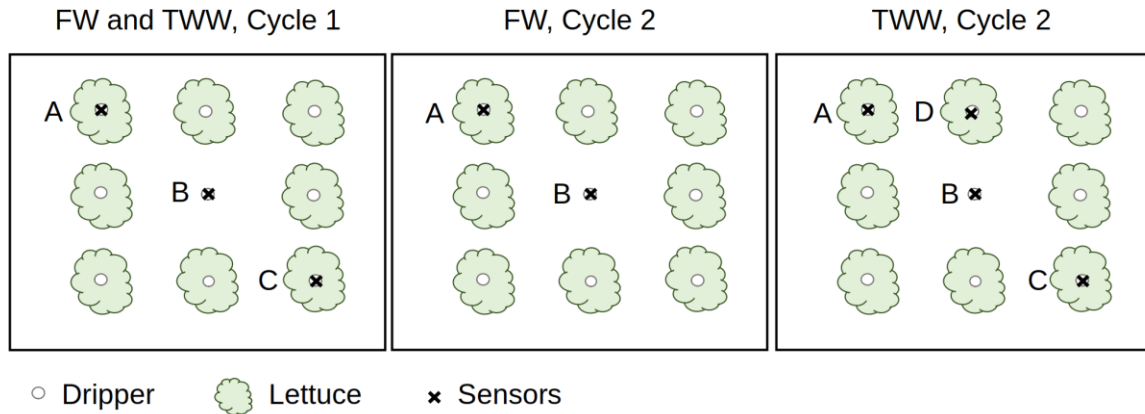
449 The soil of each bin was analysed to determine the available nitrogen (N), phosphorus (P)
450 and potassium (K) for crop growth at the beginning of each growth cycle. In addition, as
451 these nutrients are present in wastewater, the amount of N, P and K supplied through TWW
452 irrigation was estimated from analysis of the treated wastewater and typical irrigation
453 requirements. Then considering the needs of the lettuce (Berry, 2013), the nutrients already
454 present in the soil and the possible contribution from irrigation in the TWW bin, fertilisation
455 was conducted to provide for the needs of the lettuce over a cycle and ensure the same
456 level of nutrients in the TWW and FW bins. Accordingly, N was supplied to the FW bin for
457 cycle 1, P for the TWW and FW bin for cycle 2 and K for the TWW bin cycle 2.

458

459 *3.3 Soil Moisture Sensors and Lettuce Growth Monitoring*

460 For the monitoring of soil water content (SWC) 16 capacitive soil moisture sensors were
461 installed (12 sensors of model ECH20 EC5 4 sensors of model ECH20 10HS, all from
462 METER Group). Sensors were installed in pairs, at two different depths of 5cm and 20cm.
463 The sensors were positioned either under a dripper with lettuce or under a dripper without a
464 lettuce (Figure 2).

465



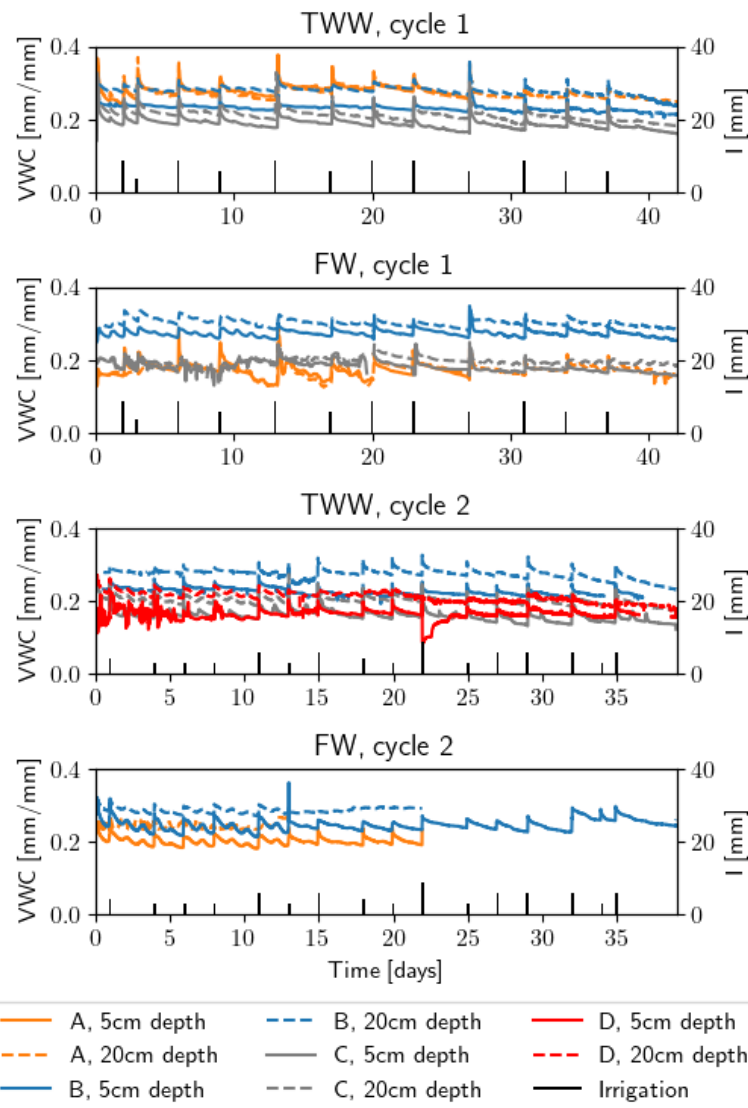
466 *Figure 2 : Position of Drippers, Lettuces and sensors in bins irrigated with freshwater (FW)*
 467 *and treated wastewater (TWW).*
 468

469 The sensors were calibrated for the soil of the experiment, according to manufacturer
 470 instructions, to obtain the parameters to convert the output of the sensors to volumetric soil
 471 water content. The sensor data was furthermore corrected to account for the effect of
 472 temperature according to the method proposed by (Cobos, 2007).
 473

474 Once a week, photos were taken of the bins and using the ImageJ software, the horizontal
 475 surface area of each lettuce was measured. Fresh and dry biomass were measured at the
 476 end of each growth cycle.
 477

478 *3.4 Model calibration and validation*

479 The data from each growth cycle was separated into calibration and validation sets, with
 480 parameters estimated with data from the 3 first weeks (days 0 to 21 for cycle 1 and days 0
 481 18 for cycle 2) and validated with data from the 3 last weeks (days 22 to 42 for cycle 1 and
 482 days 19 to 39 for cycle 2). For calibration and comparison between model and sensor
 483 output, the data from the soil moisture sensors was converted from VWC to PWC with the
 484 models' porosity parameter and then was compared to S_1 for sensors at 5cm depth and to
 485 S_2 for sensors at 20 cm depth. The weekly lettuce surface area was converted to canopy
 486 cover data by dividing the surface area of each lettuce by the soil surface area, considering
 487 that each lettuce was on a square of 1/9th of the soil bins area (i.e. 1111 cm²). The canopy
 488 cover variable C of the model was compared with the average over each soil bin of the
 489 canopy cover data. In addition, the average over each bin of the final dry weight of the
 490 lettuces was compared to the final value of the model variable B.
 491
 492



493 *Figure 3 : Data from soil moisture sensors for cycle 1 and 2, volumetric soil water content*
 494 *(VWC) [mm/mm] and irrigation volume (I [mm]) from treated wastewater (TWW) and*
 495 *freshwater (FW) irrigation. A,B,C,D denote sensor positions with A,C and D under a dripper*
 496 *with lettuce and B under a dripper without lettuce.*

497
 498

499 **4 Results and Discussion**

500

501 *4.1 Soil Water Content Measurements*

502 The volumetric soil water content as measured by the soil moisture sensors is presented in
 503 figure 3, for growth cycles 1 and 2 and for irrigation with TWW and FW. A number of sensor
 504 faults can be observed, such as problems with the recording of unphysical oscillations
 505 (sensors C, FW, cycle 1; sensors D TWW, cycle 2). Furthermore, a number of sensors
 506 malfunctioned and either recorded intermittently or produced no recording at all (sensors A,
 507 TWW, cycle 1; sensors A and B, FW cycle 2). Nonetheless, this is expected with the type of
 508 inexpensive sensors used here and has been reported as a major issue when working with
 509 cheaper sensors (Bogena 2007).

510

511 The sensor's signals follow a general pattern and two dynamics can be identified : first a fast
512 response during irrigation events and secondly, between irrigations, a slower dynamic
513 characterised by a steady decrease in VWC. During an irrigation, the sensor's signals exhibit
514 spikes corresponding to a temporary water saturation of the soil followed by a rapid
515 decrease due to drainage towards lower layers of the soil. Then, a few hours after irrigation,
516 the SWC stabilises at a value expected to represent field capacity. The second phase takes
517 place over the course of the several days between irrigations, with evapotranspiration driving
518 water losses.

519
520 The amplitude of the spikes recorded during irrigations varies, even when the same irrigation
521 volume is applied. For example, the sensor at position A, 5cm depth, in the TWW bin during
522 cycle 1, on day 6 jumps from 0.268 to 0.35 and stabilises at 0.283 but on day 13 jumps from
523 0.263 to 0.378 and stabilises at 0.301, despite both days receiving 9mm of irrigation. The
524 variations of the maximum reached can be explained by differences in the sampling time
525 during the irrigation event. Indeed, the sampling period was of 1 hour whilst irrigations lasted
526 30 minutes and therefore the measurement of the maximum reached depends on whether
527 sensors recorded during or slightly after irrigation. However, the differences in the values at
528 which VWC stabilises afterwards, i.e. field capacity, can not be as easily explained (Vories
529 2021).

530
531 In between irrigations, during the phase of slower VWC decrease, small oscillations can be
532 observed, most notably on the signal from sensors at position B in the FW bin or sensors at
533 position C in the TWW bin. Although the amplitude varies among sensors, the period is
534 always of one day with a minimum at early morning and a maximum at the end of the day.
535 This indicates that this is due to daily variations in physical conditions, such as temperature
536 which has been reported to impact measurements (Bogena 2007, Cobos 2007).

537
538 When comparing signals of the sensors within the same bin, differences can be observed in
539 the VWC measured, despite sensors being close and exposed to the same conditions. In
540 addition, for certain signals, these differences appear almost constant throughout the 6
541 weeks of each growth cycle, such as for sensors at position A and C in the TWW bin during
542 cycle 1. Furthermore, differences can be observed in the values recorded for sensors at the
543 same location but at different depths, for almost all positions, with SWC always higher in the
544 bottom soil layer and again, certain sensor signals seem to differ only by a constant value
545 (sensor C, TWW, cycle 1 and 2).

546
547 More water can be retained in the deeper layers of soil as it is less affected by
548 evapotranspiration than the topmost layer and thus a higher SWC at 20 cm depth can be
549 expected some time after an input of water. However, shortly after an irrigation event, the
550 moisture content should rapidly stabilise at field capacity and therefore, if the soil had an
551 homogeneous water holding capacity, sensors at different locations and depths should
552 record the same SWC after irrigation.

553
554 An explanation for the differences observed could be a hardware problem, such as a sensor
555 fault, or the result of actual spatial variations of the soil moisture distribution. It is not possible
556 to determine from the available measurements which of these two is the cause of the
557 observed differences and in fact it is likely a combination of both. Soil heterogeneity can
558 lead to spatial variations in VWC (Warrick 2001) but here the soil composition can be

559 supposed constant, especially considering the controlled conditions of the experiment,
560 where efforts were made to render the soil as homogeneous as possible before each cycle.
561 The local variations observed could however be explained by heterogeneities in the soil
562 structure, as previously explained, with small differences in soil compaction leading to
563 variations in porosity and thus affecting the soil water dynamics. In particular, the constant
564 differences observed between certain sensor signals indicates that a factor independent of
565 time is responsible for the spatial variations in VWC. This has led us to the suggested
566 decomposition of the measured VWC into the product of two factors, with porosity
567 accounting for spatial variations and PWC representing the time evolution of soil water
568 status.

569

570 The differences between recordings within the same bin and the various sensor faults make
571 it difficult to use such measurements directly for irrigation planning. Indeed, it is not
572 straightforward how the sensor data can be used to estimate the water holding capacity or
573 the soil water status at a given moment, which are both important to decide how much and
574 when to irrigate. This justifies the use of a model as suggested here, to correct the problems
575 with the sensor data and with the objective of irrigation decision support.

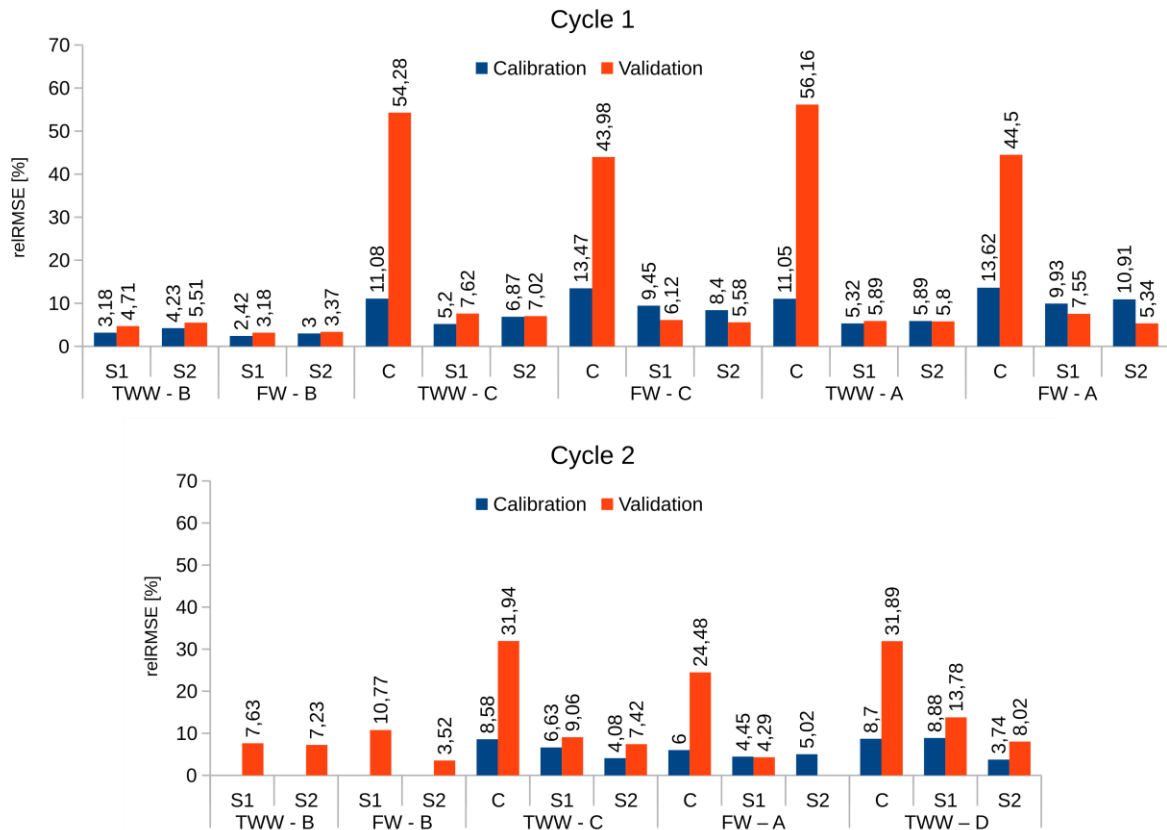
576

577 *4.2 Model calibration and validation for soil water status estimation*

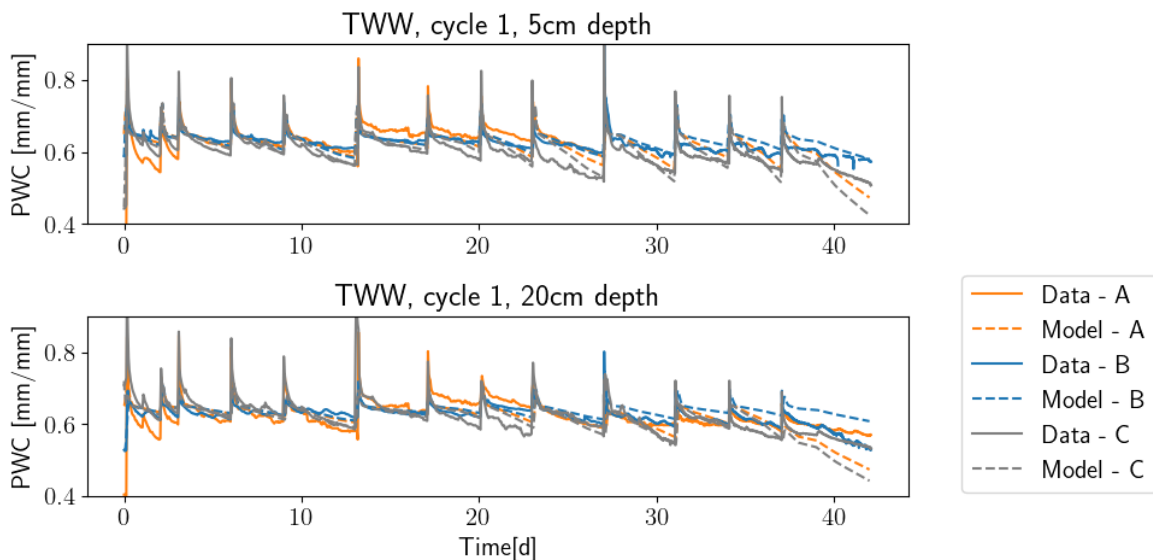
578 A first calibration, using only the first 3 weeks of data of each cycle, was designed to test the
579 performances of the model, in a context of irrigation planning. Calibration and validation
580 errors are presented in figures 4 and comparisons of model simulations and data are shown
581 in figures 5 and 6.

582

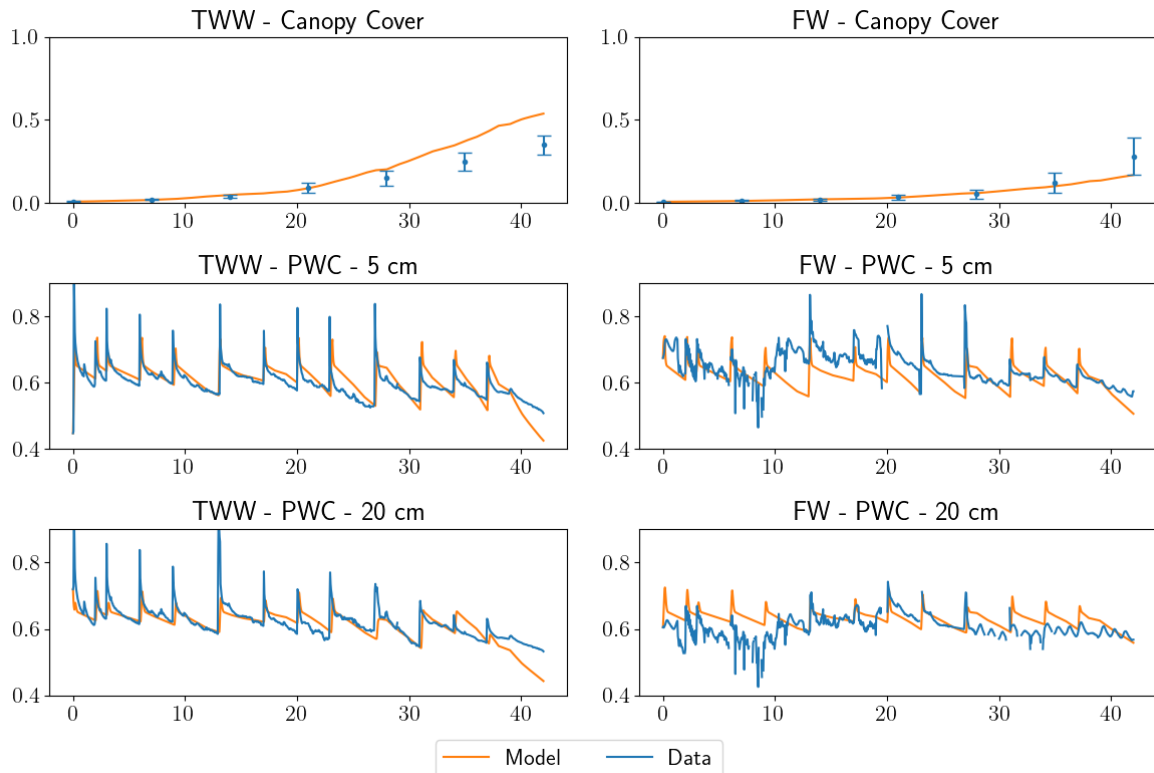
583



584 *Figure 4 : Calibration and validation relative root mean square errors (relRMSE) for cycle 1*
 585 *and 2, treated wastewater (TWW) and freshwater (FW) irrigation. A,B,C,D denote sensor*
 586 *positions with A,C,D under a dripper with lettuce and B under a dripper without lettuce.*
 587
 588



589 *Figure 5 : Comparison of sensor data and model for the treated wastewater (TWW) bin,*
 590 *cycle 1. Data is converted to pore water content (PWC) with the model's porosity parameter.*
 591 *A,B,C denote sensor positions with A,C under a dripper with lettuce and B under a dripper*
 592 *without lettuce.*
 593



594 *Figure 6: Comparison of data and model. Left : treated wastewater, cycle 1, sensor position*
 595 *C. Right : freshwater, cycle 1, sensor position A. Data for soil water is converted to pore*
 596 *water content (PWC) with the model's porosity parameter. Model parameters calibrated with*
 597 *data from the beginning to day 21.*

598

599 Overall, the model is capable of reproducing and predicting the SWC data accurately and
 600 the parameter estimation method is successful with an average calibration reIRMSE of
 601 5.85% and average validation reIRMSE of 6.8% for the SWC. Calibration is efficient and the
 602 optimization problems used to compute a set of parameters are each solved in less than 2
 603 minutes on a modern laptop computer. In particular, the strategy of reusing parameters is
 604 successful and for example, the transpiration coefficients calibrated on one data set can be
 605 used for all other simulations of a cycle. This allows the estimation of the least amount of
 606 parameters possible and results in a faster calibration. Moreover, this demonstrates the
 607 generic quality of the model and provides an extra validation of the processes represented.

608

609 Calibration was started with the sensors under drippers without lettuces as this required only
 610 the calibration of the porosity and the evaporation coefficient. The model is capable of
 611 predicting this data with very low errors, with for the first cycle an average calibration
 612 reIRMSE of 3.2% and an average validation reIRMSE of 4.19%. For the second cycle, good
 613 results were obtained without recalibration of the porosity parameter, with a mean reIRMSE
 614 of 7.28%, and this can be explained by the fact that the sensors were not moved and the soil
 615 in this area of the bins was left undisturbed between both growth cycles. However, the soil
 616 under the lettuces was disturbed after the harvest of the first cycle and sensors were
 617 repositioned, leading to a modified local soil structure which affected the porosity. Thus, for
 618 the data from sensors under lettuces, the porosity parameter had to be calibrated again for
 619 the second cycle.

620

621 After calibration of transpiration coefficients and the canopy cover growth rate, the model
 622 also simulated accurately SWC data from the sensors under lettuces with, for the first cycle,
 623 an average calibration reRMSE of 7.75% and average validation reRMSE of 6.37% and for
 624 the second cycle an average calibration reRMSE of 5.47% and average validation reRMSE
 625 of 8.14%. For the canopy cover, the model achieves low calibration errors, with a mean
 626 reRMSE of 12.3% for the first cycle and of 7.76% for the second cycle. The model is less
 627 accurate during the validation period, in particular in the first cycle with an average reRMSE
 628 of 49.73% but with a better performance for the second cycle with an average reRMSE of
 629 29.44%. However despite these errors, the model is capable of reproducing the general
 630 trend of the canopy growth sufficiently well to obtain very good predictions of the SWC which
 631 is the primary objective here.

632
 633 These results also show that the model is capable of dealing with sensor faults and provides
 634 a data filtering method. Indeed, for the first cycle, the SWC data from sensors at position C
 635 in the FW bin was of bad quality during the calibration period. Nonetheless, this data was
 636 used to estimate the porosity parameters associated with these sensors as well as the
 637 canopy growth parameter for the FW water quality. Despite the sensor fault, calibration was
 638 successful as shown by the low error obtained during the validation period, for which the
 639 data was of better quality. Incidentally, the difference in data quality between the beginning
 640 and end periods of cycle 1 in the FW bin likely explains why validation errors are lower than
 641 calibration errors for sensors A and C. During the second cycle, sensor D in the TWW bin,
 642 recorded an extremely noisy signal but again the calibration method was capable of dealing
 643 with this fault and porosity was correctly estimated, yielding low validation errors.
 644 Furthermore, in the case of a malfunction resulting in no more recordings, such as sensor A
 645 in the FW bin during the second cycle, the model provides a means of estimating the SWC.

646
 647 Using the calibrated porosity parameters, the VWC data can be converted to PWC and
 648 much less spatial variability can be observed in the converted sensor signals and in the
 649 simulations. To compare signals of different sensors, the average relative difference is
 650 computed. Denoting θ_A and θ_B the signals of 2 sensors and $\bar{\theta}_A$ the mean of a signal, then the
 651 relative difference is:

$$652 \frac{|\theta_A - \theta_B|}{\bar{\theta}_A} \quad (20)$$

653
 654 From this, the average is then computed over the time interval of interest. The average of
 655 the relative difference between signals from sensors A and C in the TWW bin, cycle 1, is
 656 30.07% in the top and 22.01% in the bottom layer when comparing the signals of VWC.
 657 However, once converted to PWC, these differences drop to 5.4% in the top and 5.52% in
 658 the bottom. Differences between top and bottom layers are also reduced and in the case of
 659 sensors at position C in the TWW bin, cycle 1, the mean difference between the two layers is
 660 11.5% in VWC but only 3.5% in PWC. In addition, the difference between PWC under
 661 drippers with or without lettuce is also small at the beginning but becomes more important
 662 later in the cycle, when the lettuce has a greater impact on water dynamics.

663
 664 The porosity parameters estimated are presented in figure 7 and table 3. It can be noticed
 665 that the porosity of the bottom layer is always greater or equal than in the top layer.
 666 Assuming that differences in porosity are responsible for the spatial variations measured, the
 667

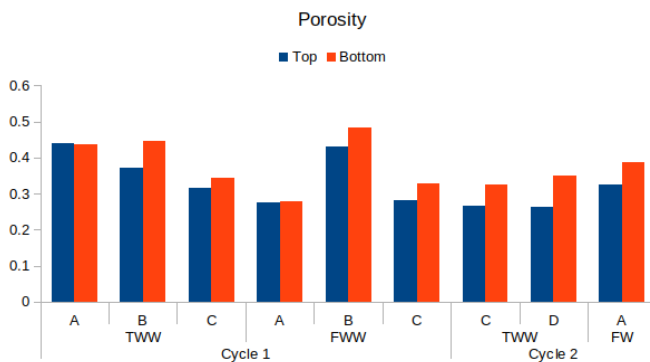
668 approach presented here can also be seen as a method to estimate the spatial variability of
 669 the soil water holding capacity. Indeed, the porosity allows to convert PWC to VWC so that
 670 the height corresponding to the field capacity of a layer is ϕZS_{fc} . Therefore, since the field
 671 capacity is assumed constant when expressed relative to pore volume, the mean and
 672 standard deviation of the field capacity is the mean and standard variation of porosity
 673 multiplied by ZS_{fc} . In this present study, this gives an average field capacity between 20.74
 674 mm and 25.09 mm with a standard deviation between 3.51 mm and 5.2 mm, which gives
 675 valuable information on the spatial variability of soil water holding capacity and is directly
 676 usable for irrigation planning.

677
 678

Table 3 : Statistics of porosity parameters estimated.

	Cycle 1		Cycle 2	
	Mean	Std	Mean	Std
Top	0.352	0.072	0.319	0.054
Bottom	0.386	0.08	0.393	0.057

679
 680



681
 682 *Figure 7 : Porosity parameters calibrated from sensor data. Treated wastewater (TWW) and*
 683 *freshwater (FW) irrigation. A,B,C,D denote sensor positions with A,C,D under a dripper with*
 684 *lettuce and B under a dripper without lettuce.*

685

4.3 Full cycle calibration for analysis

686
 687 The lettuces biomass were measured only at the end of cycle and therefore to calibrate the
 688 biomass growth rate parameter, it was necessary to use data from an entire cycle.
 689 Moreover, as the errors on the canopy cover were more important during the second part of
 690 both cycles, it was also decided to estimate r_G again in order to reproduce the data more
 691 accurately with the objective of using this calibration for the analysis of the experiment.
 692 The calibration was successful, with an overall reRMSE of 22.18% for the canopy cover and
 693 2.06% for the biomass (Figure 8).

694

695 Figures 9, 10 and 11 compare the data and model simulations of the canopy cover and dry
 696 biomass. Differences between bins with irrigation of FW and TWW can be noted during the
 697 first cycle mainly, both on the biomass and canopy growth. Interestingly, these differences
 698 can be reproduced with the model with differences in only the canopy growth rate whilst the
 699 evapotranspiration coefficients and biomass growth rate were the same for both water
 700 qualities. The canopy growth rate therefore translates the impact on lettuce growth of the
 701 different conditions. Furthermore, the parameters estimated from the two different

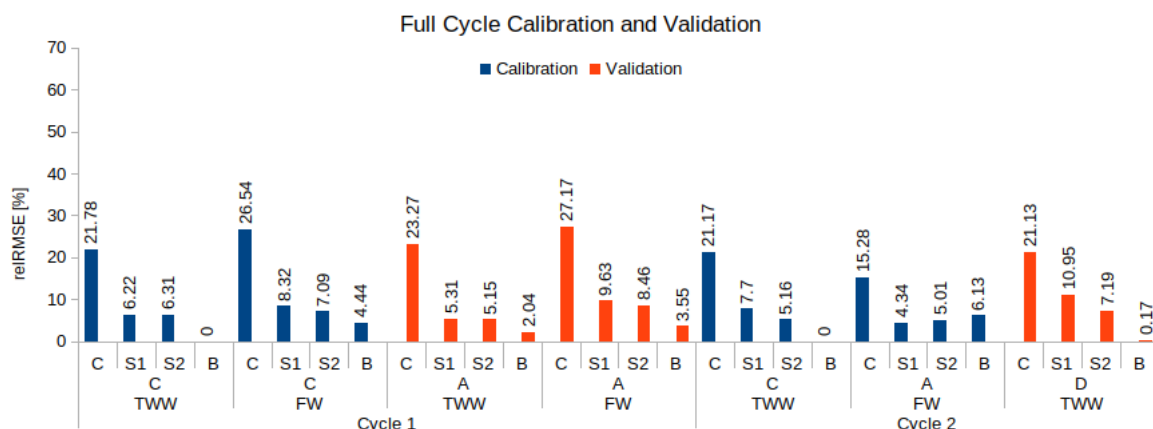
702 calibrations can be contrasted to see if growth was different at the beginning and end of the
 703 cycles, as presented in table 4. For the first cycle, comparing calibrated parameters with
 704 data from the first 21 days or from the full cycle, shows that for the FW bin, lettuces had a
 705 slow start with a lower growth rate at the beginning. However, the opposite happened for the
 706 TWW bin for cycle 1 and 2 as well as for the FW bin for cycle 2. This can be related to
 707 fertilisation of the FW bin occurring only on day 10 of the first cycle, whereas for the TWW,
 708 nutrients were added to the soil with each irrigation. Therefore the slower start of the FW
 709 lettuces can be explained in part by a nutrient deficit at the beginning of the cycle, with an
 710 increased growth rate after fertilisation. This is further supported by the fact that during the
 711 second cycle, when both bins were sufficiently fertilised over the entire cycle, lettuces had
 712 the similar canopy growth rates for both water qualities.

714 The different water flows of the soil crop system can be computed from the model simulation
 715 and are presented in Figure 12. During the second cycle, irrigation was done with smaller
 716 but more frequent events and the positive impact of this practice can be clearly seen.
 717 Indeed, leakage losses were between 43 and 52 % of irrigation in cycle 1 but decreased to
 718 between 17 and 28% for cycle 2. Furthermore, despite a decrease in total irrigation of 17mm
 719 from the first to the second cycle, the total evapotranspiration increased by 6 mm in the
 720 TWW bin and by 15 mm in the FW bin. This is the result of greater evaporation due to higher
 721 temperatures and increased transpiration from greater growth of the lettuces during the
 722 second cycle.

725 *Table 4 : Canopy growth rate parameters calibrated*

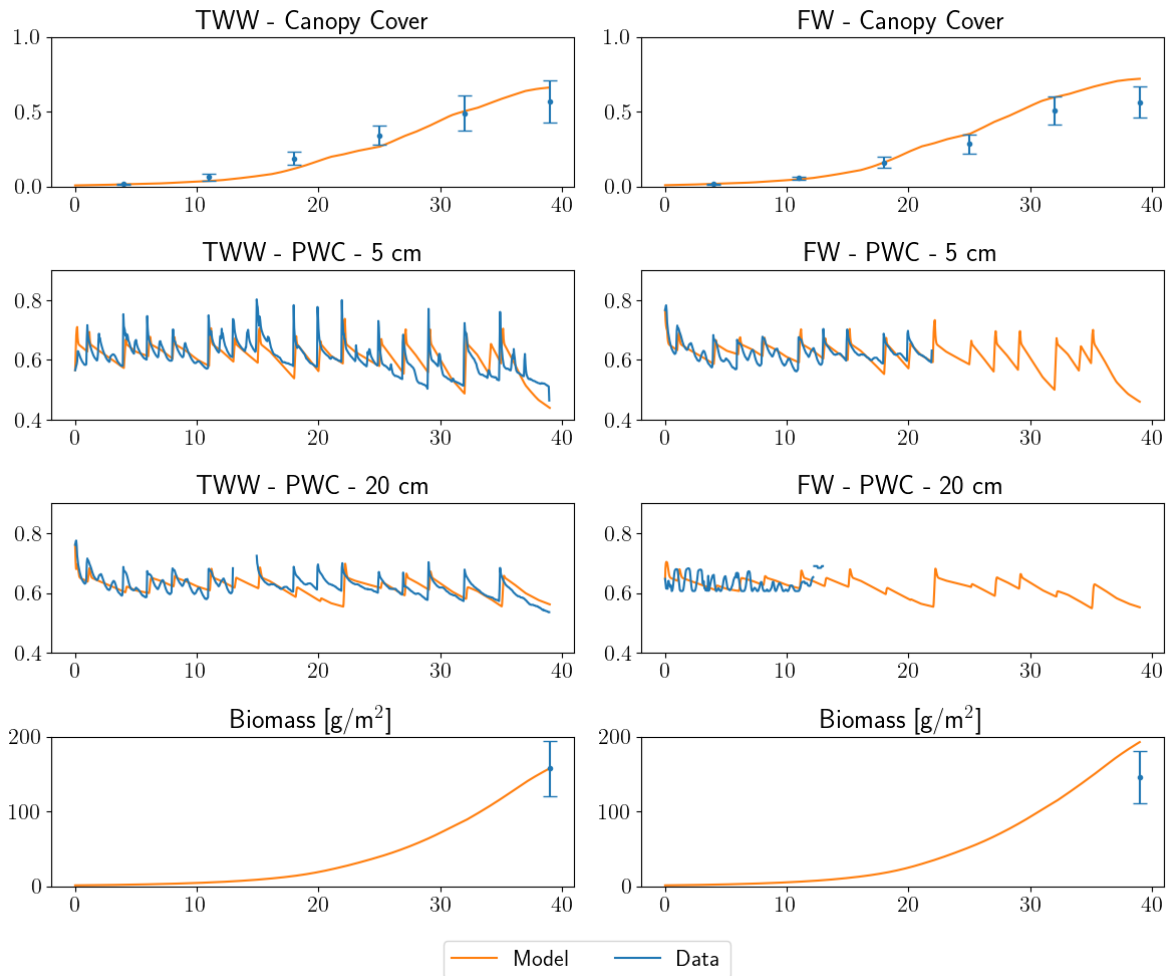
	Irrigation water quality	First calibration	Full cycle calibration
Cycle 1	TWW	0.0257	0.0226
	FW	0.01638	0.0184
Cycle 2	TWW	0.05544	0.04631
	FW	0.0497	0.0457

726
727

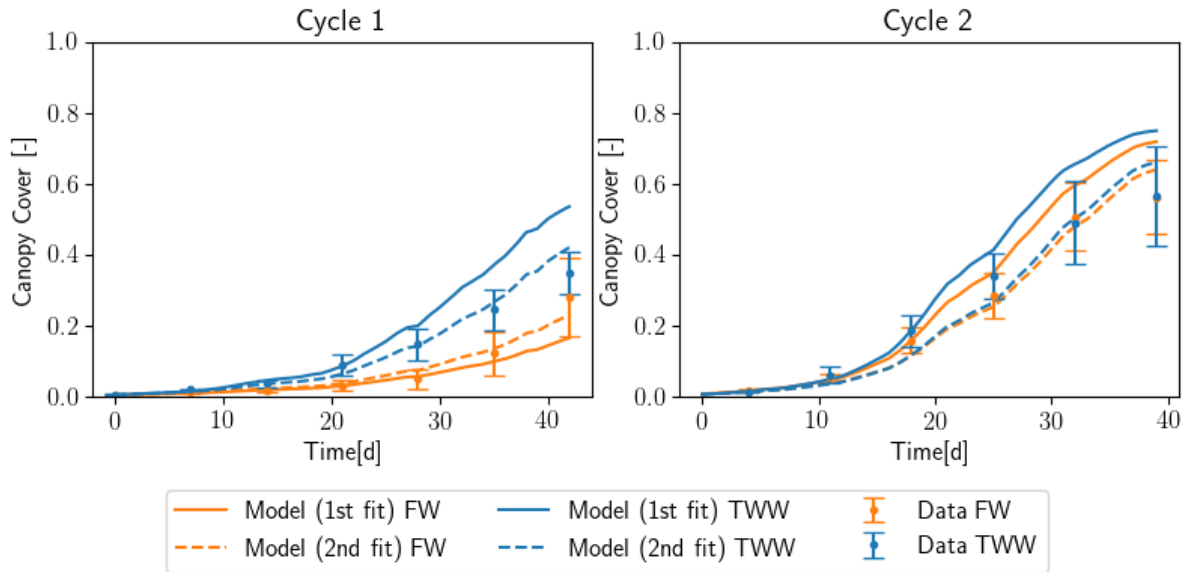


728
729 *Figure 8 : Calibration and validation errors for 2nd calibration of canopy cover and biomass*
 730 *growth rates with data of entire cycle. Treated wastewater (TWW) and freshwater (FW)*
 731 *irrigation. A,B,C,D denote sensor positions with A,C,D under a dripper with lettuce and*
 732 *under a dripper without lettuce.*

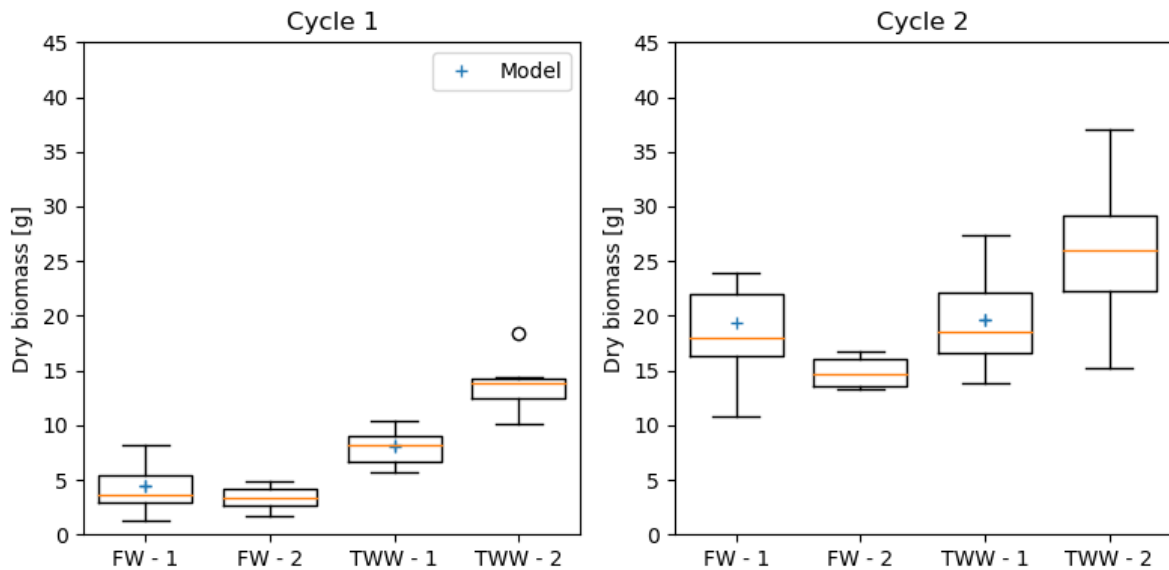
733



734 *Figure 9 : Comparison of data and model with canopy cover and biomass growth rate*
 735 *parameters calibrated with data from the entire cycle. Left : TWW, cycle 2, sensor position C.*
 736 *Right : FW, cycle 2, sensor position A. Data for soil water is converted to PWC with the*
 737 *model's porosity parameter.*
 738
 739
 740

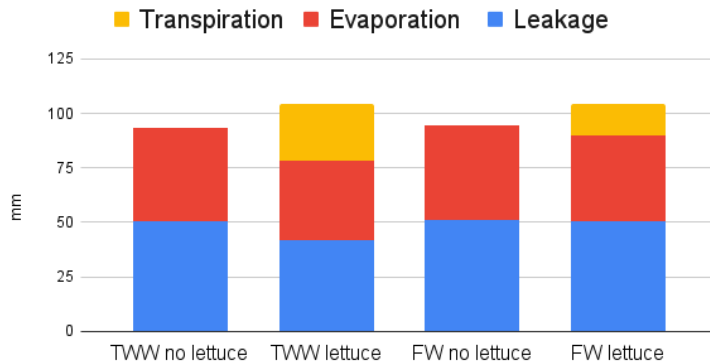


741
 742 *Figure 10 : Comparison of Canopy cover data and model. Data is average per bin with error*
 743 *bars representing one standard deviation. For the model, the first fit was done using only*
 744 *data from the first 3 weeks of each cycle and the 2nd fit was done using data from the entire*
 745 *cycle.*
 746
 747

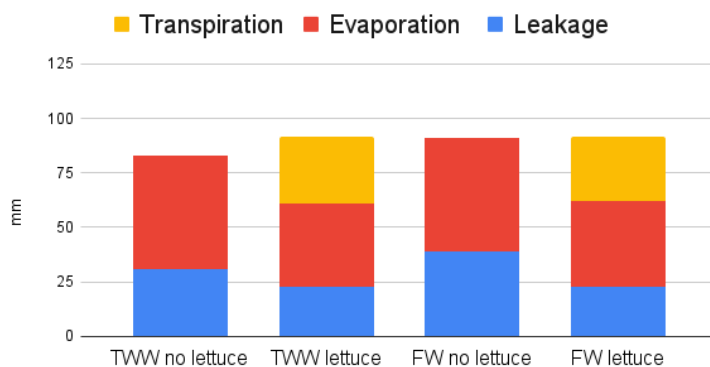


748
 749 *Figure 11 : Dry mass [g] of lettuce at harvest per bin with the soil water sensors positioned in*
 750 *bins labelled 'FW - 1' and 'TWW - 1'. Bins labelled 'FW - 2' and 'TWW - 2' are replicates for*
 751 *which soil moisture sensor data was not available. Simulated final dry biomass is also*
 752 *shown, with the biomass growth parameter calibrated with data from bin 'TWW - 1'.*
 753
 754
 755

Cycle 1



Cycle 2



756 *Figure 12 : Water flows computed from model for treated wastewater (TWW) and freshwater*
 757 *(FW) bins.*

758
 759

760 5 Conclusions

761 The results of this study show that a simple model can be a valuable tool to complement
 762 sensors in accurately estimating the water status of a soil crop system. Indeed, the model
 763 and the calibration method are successful at taking into account the spatial variations in the
 764 SWC measured, whether they are caused by sensor fault or actual variations in soil water. In
 765 particular, this work provides a means to obtain a single value representing the soil water
 766 status in the vicinity of a sensor that can be used for irrigation planning.

767

768 The simplicity of the model translates into fast calibration and simulations, which are
 769 essential for practical use. A disadvantage of a simpler model as the one presented here, is
 770 that not all processes involved in crop growth or soil water dynamics are included, leading to
 771 a model which can be expected to be less generic. However, trying to take into account all
 772 effects to obtain a generic model can lead to extremely complex models which turn out to be
 773 very difficult to calibrate efficiently. In general, developing models for real world application
 774 implies making trade-offs between model complexity for genericity and simplicity for
 775 efficiency. Access to online measurements has an impact on these trade offs, as data can be
 776 used to calibrate a simple model to each specific situation, achieving genericity with a
 777 simpler representation.

778
 779

780 **Acknowledgements**

781 These results are part of the JPI project Control4reuse (<http://control4reuse.net>) financed by
782 the French Research National Agency under the contract ANR-18-IC4W-0002.

783

784

785 **References**

786

787 Abioye, E. A., Abidin, M. S. Z., Mahmud, M. S. A., Buyamin, S., Ishak, M. H. I., Abd
788 Rahman, M. K. I., ... & Ramli, M. S. A. (2020). A review on monitoring and advanced control
789 strategies for precision irrigation. *Computers and Electronics in Agriculture*, 173, 105441.

790

791 Ait-Mouheb, N., Mange, A., Froment, G., Lequette, K., Bru-Adan, V., Maihol, J. C., ... &
792 Wery, N. (2022). Effect of untreated or reclaimed wastewater drip-irrigation for lettuces and
793 leeks on yield, soil and fecal indicators. *Resources, Environment and Sustainability*, 8,
794 100053.

795

796 Ait-Mouheb, N., Bahri, A., Thayer, B. B., Benyahia, B., Bourrié, G., Cherki, B., ... & Harmand,
797 J. (2018). The reuse of reclaimed water for irrigation around the Mediterranean Rim: a step
798 towards a more virtuous cycle?. *Regional Environmental Change*, 18(3), 693-705.

799

800 Allen, R. G., Pereira, L. S., Raes, D., & Smith, M. (1998). FAO Irrigation and drainage paper
801 No. 56. *Rome: Food and Agriculture Organization of the United Nations*, 56(97).

802

803 Berry D. (2013). Culture biologique des laitues. [https://extranet-ain.chambres-
804 agriculture.fr/fileadmin/user_upload/National/FAL_commun/publications/Auvergne-Rhone-
805 Alpes/AB_Culture_biologique_laitues_2013.pdf](https://extranet-ain.chambres-agriculture.fr/fileadmin/user_upload/National/FAL_commun/publications/Auvergne-Rhone-Alpes/AB_Culture_biologique_laitues_2013.pdf), (Accesed 18-2-2021)

806

807 Bogen, H. R., Huisman, J. A., Oberdörster, C., & Vereecken, H. (2007). Evaluation of a
808 low-cost soil water content sensor for wireless network applications. *Journal of Hydrology*,
809 344(1-2), 32-42

810

811 Brisson, N., Gary, C., Justes, E., Roche, R., Mary, B., Ripoche, D., ... & Sinoquet, H. (2003).
812 An overview of the crop model STICS. *European Journal of agronomy*, 18(3-4), 309-332.

813

814 Cheviron, B., Vervoort, R. W., Albasha, R., Dairon, R., Le Priol, C., & Mailhol, J. C. (2016). A
815 framework to use crop models for multi-objective constrained optimization of irrigation
816 strategies. *Environmental Modelling & Software*, 86, 145-157.

817

818 Clapp, R. B., & Hornberger, G. M. (1978). Empirical equations for some soil hydraulic
819 properties. *Water resources research*, 14(4), 601-604.

820

821 Cobbenhagen, A. T. J. R., Antunes, D. J., van de Molengraft, M. J. G., & Heemels, W. P. M.
822 H. (2021). Opportunities for control engineering in arable precision agriculture. *Annual
823 Reviews in Control*, 51, 47-55.

824

825 Cobos, D., & Campbell, C. (2007). Correcting temperature sensitivity of ECH2O soil
826 moisture sensors. *Appl. Note. Decagon Devices, Pullman, WA*.

827

828 Feng, G., & Sui, R. (2020). Evaluation and calibration of soil moisture sensors in undisturbed
829 soils. *Transactions of the ASABE*, 63(2), 265-274.

830

831 Khalil, H. (2015) *Nonlinear Control*, Global Edition, Pearson, 394 pages.

832

833 Laio, F., Porporato, A., Ridolfi, L., & Rodriguez-Iturbe, I. (2001). Plants in water-controlled
834 ecosystems: active role in hydrologic processes and response to water stress: II.
835 Probabilistic soil moisture dynamics. *Advances in water resources*, 24(7), 707-723.

836

837 Mailhol, J. C., Ruelle, P., Walser, S., Schütze, N., & Dejean, C. (2011). Analysis of AET and
838 yield predictions under surface and buried drip irrigation systems using the Crop Model
839 PILOTE and Hydrus-2D. *Agricultural Water Management*, 98(6), 1033-1044.

840

841 Pelak, N., Revelli, R., & Porporato, A. (2017). A dynamical systems framework for crop
842 models: Toward optimal fertilization and irrigation strategies under climatic variability.
843 *Ecological Modelling*, 365, 80-92.

844

845 Pereira, L. S., Paredes, P., & Jovanovic, N. (2020). Soil water balance models for
846 determining crop water and irrigation requirements and irrigation scheduling focusing on the
847 FAO56 method and the dual Kc approach. *Agricultural water management*, 241, 106357.

848

849 Rodríguez-Iturbe, I., & Porporato, A. (2007). *Ecohydrology of water-controlled ecosystems:
850 soil moisture and plant dynamics*. Cambridge University Press.

851

852 Šimůnek, J., M. Šejna, and M. Th. van Genuchten, New Features of the Version 3 of the
853 HYDRUS (2D/3D) Computer Software Package, *Journal of Hydrology and Hydromechanics*,
854 66(2), 133-142, doi: 10.1515/johh-2017-0050, 2018.

855

856 Steduto, P., Hsiao, T. C., Raes, D., & Fereres, E. (2009). AquaCrop—The FAO crop model
857 to simulate yield response to water: I. Concepts and underlying principles. *Agronomy
858 Journal*, 101(3), 426-437.

859

860 Stetson, L. E., & Mecham, B. Q. (Eds.). (2011). *Irrigation*. Irrigation Association.

861

862 Sui, R., & Vories, E. D. (2020). Comparison of sensor-based and weather-based irrigation
863 scheduling. *Applied Engineering in Agriculture*, 36(3), 375-386.

864

865 Villalobos, F. J., & Fereres, E. (Eds.). (2016). *Principles of agronomy for sustainable
866 agriculture* (p. 443457). New York, NY, USA:: Springer.

867

868 Vories, E., & Sudduth, K. (2021). Determining sensor-based field capacity for irrigation
869 scheduling. *Agricultural Water Management*, 250, 106860.

870

871 Walter, E., & Pronzato, L. (1997). *Identification of parametric models: from experimental
872 data*. Springer Verlag.

873

874 Warrick, A. W. (2001). *Soil physics companion*. CRC press.

875